УДК 544.034:546.26

Features of carbon diffusion during plasma electrolytic carburising of low-carbon steels

Особенности диффузии углерода при плазменном электролитическом науглероживании низкоуглеродистых сталей

S. Y. Shadrin* *, S. A. Kusmanov, T. A. Kovrizhnykh, P. N. Belkin
С. Ю. Шадрин* *, С. А. Кусманов, Т. А. Коврижных, П. Н. Белкин

Kostroma State University, Dzerzhinsky Str., 17, Kostroma, 156005, Russia
* syushadrin@yandex.ru

Костромской государственный университет, Россия, 156005, Кострома, ул. Дзержинского, 17
* syushadrin@yandex.ru

ABSTRACT

This work is devoted to evaluation of the diffusion coefficient of carbon using the thickness of the martensitic layer after plasma electrolytic carburizing in various electrolytes followed by quenching. The carbon diffusion coefficient was calculated using the solution of the diffusion equation for a semi-infinite body according to the thickness of the martensitic layer which was measured by means of an optical microscope. The effective diffusion coefficients of carbon in the structure of mild steel containing oxide and martensitic layers are determined. The maximum diffusion coefficient at a carburising temperature of 900 °C is 2.3×10^{-7} cm^2/s for treatment in an acetone-based electrolyte for 1 min. The obtained values were comparable with the calculation results for the thickness of the pearlite layer after anodic plasma electrolytic carburising as well as data of measurements of the distribution of carbon concentration in the carburised layer after cathodic saturation. The influence of the oxide layer inhibiting the diffusion of carbon and the possibility of controlling its thickness by varying the concentration of ammonium chloride, which provides anodic dissolution of steel, were confirmed. It has been established that the published values of the coefficients of carbon diffusion during plasma electrolytic carburising relate to various structures whose characteristics and properties depend on the composition of the working electrolytes and processing conditions.

KEYWORDS

Electrolysis plasma; carburising; diffusion coefficient; steel.

АННОТАЦИЯ

Посвящена оценке коэффициента диффузии углерода с использованием толщины мартенситного слоя после плазменной электролитической цементации в различных электролитах с последующим гашением. Коэффициент диффузии углерода был рассчитан путем решения задачи диффузии для полубесконечного тела в зависимости от толщины мартенситного слоя, который измерялся с помощью оптического микроскопа. Эффективные коэффициенты диффузии углерода в воздухе определяли по структуре мягкой стали, содержащей оксидные и мартенситные слои. Максимальный коэффициент диффузии при температуре науглероживания 900 °C составляет $2{,}3 \times 10^{-7}$ см^2/с для обработки в электролите на основе ацетона в течение 1 мин. Полученные значения были сопоставимы с расчетными результатами по толщине перлитного слоя после анодно-плазменного электролитического науглероживания, а также с данными измерений распределения концентрации углерода в науглероживаемом слое после катодного насыщения. Было подтверждено влияние оксидного слоя, ингибирующего диффузию углерода и возможность регулирования его толщины путем изменения концентрации хлорида аммония, который обеспечивает анодное растворение стали. Было установлено, что опубликованные значения коэффициентов диффузии углерода при плазменном электролитическом науглероживании относятся к различным конструкциям, характеристики и свойства которых зависят от состава рабочей среды электролита и условий обработки.

КЛЮЧЕВЫЕ СЛОВА

Электролизная плазма; науглероживание; коэффициент диффузии; сталь.

Introduction

Plasma electrolytic carburising (PEC) of metals and alloys attracts the attention of researchers with new technological capabilities. These include reduction in processing time to several minutes, combination with hardening without reheating, the convenience of performing local processing of individual areas of the component, and the use of inexpensive equipment [1, 2]. The saturating medium during PEC is the

vapour-gaseous envelope (VGE) which is formed around the workpiece due to boiling of the electrolyte and has sufficient electrical conductivity. High-speed PEC provides an increase in wear resistance of steel H13 [3], AISI 304 [4], T8 [5] and aluminium [6], as well as the corrosion resistance of commercial pure titanium [7], titanium alloy Ti-48Al-2Cr-2Nb [8] and aluminium alloy 6082 [9].

A specific feature of the PEC is a more complex three-phase system (electrolyte solution, VGE, metal electrode) compared to traditional carbon saturation from a solid or gas phase [10]. Firstly, the saturation temperature depends on the heating voltage, the polarity of the workpiece, the composition of the electrolyte, its temperature and the hydrodynamic conditions in the electrolyser. Secondly, the diffusion saturation with carbon is further complicated by the inevitable chemical and electrochemical reactions, as well as by the action of electric discharges in the VGE. These PEC features determine the kinetics of carbon saturation of steels obtained by various authors.

Cathodic PEC occurs in more difficult conditions than anodic one. Electric discharges in VGE create unsteady heat sources, which makes it difficult to measure the temperature directly in the carburised material, where carbon diffusion takes place. For these reasons, the effect of the PEC duration on the layer thickness is different. For example, the increasing time dependence of the thickness of the carburised layer during the treatment of pure iron in a glycerol-based electrolyte is not parabolic [11], therefore, the surface carbon concentration during saturation cannot be considered constant. However, the saturation of mild steel with carbon in a 25 wt.% solution of potassium acetate in glycerol leads to a parabolic dependence of the layer thickness on the processing time [12]. It can be assumed that a constant concentration of carbon on the surface of the steel is achieved by additional stabilization of the conditions in the VGE owing to the use of two current sources (direct and high-frequency current). A surface carbon concentration of 1.4 wt.% is determined for PEC in a solution of potassium acetate in glycerol at 950 °C and a frequency of 350 Hz [13]. The carbon potential is also measured at the PEC of low-carbon steel (900 °C, 15 min) in an aqueous solution containing 10 wt.% sodium carbonate and 20 wt.% ethanol equal to 0.7 wt.% [14]. The temperature conditions and structure of the layers obtained in these examples reveals that carbon diffuses in austenite.

A more complex structure is formed during the cathodic PEC of T8 high carbon steel in an 80 wt.% glycerol solution with the addition of potassium chloride [15]. Saturation with carbon at 380 V for 3 min results in the formation of a structure containing two layers. The outer layer with 30 μm thick is carbon-enriched cementite, in which the carbon concentration changes from (9–15) wt.% on the surface to (6.5–7.0) wt.% at a depth of 30 μm according to energy dispersive spectroscopy. In the second layer, called diffusive one, the carbon content decreases and reaches the initial 0.8 wt.% at a depth of 70 microns. In this case, the average carbon diffusion coefficient is $2.72 \cdot 10^{-7}$ cm^2/s at 380 V and a PEC temperature of 800 °C. Note that the switch-off of voltage after the PEC in an 80 wt.% glycerol solution does not lead to quenching and the formation of martensite [16]. A possible cause may be an increased viscosity of this solution. Also, the carbon potential of the sodium carbonate solution is found to be (0.6–0.7) wt.% [17].

The anode PEC occurs under almost stationary conditions without electric discharges in the VGE, which enables to measure the temperature of a workpiece or sample with acceptable accuracy. As a rule, the dependence of the thickness of the martensitic layer after PEC followed by quenching on the saturation time is parabolic [18].

The carbon potential of electrolytes at the anode PEC is estimated using various methods. The layer structure contains the portions of cementite in the form of a grid, the area of which did not exceed 2%. In this case, the carbon potential of VGE is taken equal to 0.9 wt.%. The potential of 0.8 wt.% corresponds to the absence of a cementite network and ferrite grains. The appearance of ferrite grains occupying an area of up to 10% of the area of perlite grains permits to estimate the carbon potential as 0.7 wt.% [19].

The simplest example of estimating the carbon diffusion coefficient is the experimental measurement of the weight a thin wire of low-carbon steel after its anodic PEC in a solution of glycerol and ammonium chloride at (180–240) V [20]. A theoretical calculation of the average carbon concentration in the wire, based on the solution of the diffusion equation with a constant concentration of carbon on the surface allows

obtaining the average diffusion coefficient of $(1.0\pm0.2) \cdot 10^{-7}$ cm^2/s. The PEC temperature is not measured, but the identification of areas of coarse-grained martensite at the PEC voltage of 240 V confirms a certain austenitisation of the surface layer.

The carbon diffusion coefficient at the anodic PEC is also estimated from the measurements of the average carbon concentration at a given depth using emission spectral analysis [21]. A well-known solution of the diffusion equation for a semi-infinite body:

$$\frac{C-C_0}{C_S-C_0}=\operatorname{erfc}\left(\frac{x}{2\sqrt{Dt}}\right), \quad (1)$$

modified by the introduction of an average volume concentration:

$$\overline{C}=\frac{1}{V}\int_V CdV=C_0+(C_S-C_0)\int_0^l \operatorname{erfc}\left(\frac{x}{2\sqrt{Dt}}\right)=$$
$$=C_0+(C_S-C_0)F(D),$$
$$F(D)=\frac{1}{\sqrt{\pi}}\left(1-\exp\left(-\frac{l^2}{4Dt}\right)\right)\frac{2\sqrt{Dt}}{l}+\operatorname{erfc}\left(\frac{l}{2\sqrt{Dt}}\right), \quad (2)$$

where C is the carbon concentration at depth x, C0 is the initial carbon concentration, CS is the carbon concentration on the surface of the sample, D is the carbon diffusion coefficient in steel, t is time, erfc (x) is an additional error function, l is the depth of determining the volume carbon concentration. Then, in the expression (1), the carbon concentration on the surface of the CS sample can be replaced by its average value in depth, which gives:

$$C=C_0+\frac{(\overline{C}-C_0)}{F(D)}\operatorname{erfc}\left(\frac{x}{2\sqrt{Dt}}\right). \quad (3)$$

The carbon content in the pearlite layer being 0.76 wt.% is chosen to determine the diffusion coefficient [22]. The depth of the layer is determined optically. The diffusion coefficient of carbon is $1.29 \cdot 10^{-8}$ cm^2/s at 900 °C. In the same work, the effect of the electrolyte composition on the characteristics of carbon diffusion in steel is discovered which is explained by a change in the composition of its surface layer owing to the formation of iron oxides inhibiting carbon transfer.

Determining the thickness of a pearlite layer requires an additional operation of tempering or cooling the sample in air after PEC. In the latter case, incomplete hardening of carburised steel is not excluded. The aim of this article is to verify an alternative version for estimating the diffusion coefficient of carbon using the thickness of the martensitic layer, which is easily visually determined after etching of the sample or by the distribution of microhardness in the layer. In this case, the carbon concentration at the boundary of the martensitic layer is taken to be 0.26 wt.% [22]. The carbon diffusion coefficient is found by numerically solving equation (3) using known estimates of the carbon potential of VGE formed in electrolytes of various compositions.

1. Materials and equipment

Cylindrical samples of low-carbon steel (0.1 wt.% C) with a height of 20 mm and a diameter of 10 mm were subjected to anodic PEC. All samples were cleaned with sandpaper to a surface roughness of Ra 1.01 μm and washed with ultrasound in acetone before processing. The PEC was carried out in a cylindrical axisymmetric electrolyser with a longitudinal flow around the samples with electrolyte supplied through a nozzle located in the bottom of the chamber. The electrolyte was overflowed the upper edge of the chamber into a tray and further pumped through the heat exchanger at a flow rate of 3 l/min. The electrolyte flow rate was determined using a float rotameter RMF-0.16. The electrolyte temperature was measured with an MS-6501 digital thermometer with TP – 01 fast response thermocouples and maintained at (20±1) °C.

After applying voltage, the samples were immersed in the electrolyte to a depth equal to the height of the samples. After PEC, the samples were quenched in the electrolyte from the saturation temperature. The voltage value was recorded using an LM-1 voltmeter. The current was controlled using an MS8221 multimeter. The samples temperature was determined by the MS8221 multimeter and the M89–K1 thermocouple with an accuracy of 2% in the range 400–1000 °C. The heating temperature of the samples varied from 800 to 1000 °C, the processing time was 1, 3 and 7 minutes. An aqueous solution of ammonium chloride and one of the carbon-containing components: acetone, ethylene glycol, glycerol, sucrose, ethyl and isopropyl alcohol were used as a working electrolyte. The concentration of

carbon-containing components of the electrolyte was 10 wt.%, the concentration of ammonium chloride was also 10 wt.%.

The structure of the surface layer of the samples was studied using an EC METAM RV-21 optical microscope after polishing and etching (4 wt.% solution of nitric acid in ethanol) for 5–10 s.

2. Results and its discussion

First of all, we evaluate the carbon potential of glycerol-based electrolytes and the diffusion coefficient of carbon over the thickness of the martensitic layer using the previously published data [21] and compare them with the data obtained for the pearlite layer (Table 1).

Data of Table 1 show that the obtained values of the diffusion coefficient are close, while the carbon potential practically coincides for a heating temperature of 1000 °C. Hence, the minimum concentration in the martensitic layer can be used as a characteristic carbon concentration. This layer is well detected in the images of the structure; therefore, determining its thickness is not difficult (Fig. 1).

Table 2 contains the experimental data on the anodic PEC of low-carbon steel in electrolytes of various compositions. The carbon potentials of electrolytes are determined by measuring the surface concentration of carbon using spectroscopy of proton nuclear backscattering [23].

Table 1
Таблица 1

Conditions and results of evaluating the diffusion coefficient of carbon and the carbon potential of glycerol electrolyte during anodic PEC [21]. Nomenclature: C_{gl} is glycerol concentration, C_{ch} is ammonium chloride concentration, T is PEC temperature, t is PEC duration, δ_p is pearlite layer thickness, δ_m is martensitic layer thickness, C_V is volumetric carbon concentration in a layer of 75 microns thick, D_1 is carbon diffusion coefficient (pearlite calculation), C_{S1} is surface carbon concentration (pearlite calculation), D_2 is carbon diffusion coefficient (martensite calculation), C_{S2} is surface carbon concentration (martensite calculation).

Условия и результаты оценки коэффициента диффузии углерода и углеродного потенциала глицеринового электролита при анодной плазменной электролитической цементации [21]. Номенклатура: C_{gl} – концентрация глицерина, C_{ch} – концентрация хлорида аммония, T – температура цементации, t – продолжительность PEC, δ_p – толщина слоя перлита, δ_m – толщина мартенситного слоя, C_V – объемная концентрация углерода в слое толщиной 75 микрон, D_1 – коэффициент диффузии углерода (расчет по перлиту), C_{S1} – поверхностная концентрация углерода (расчет перлита), D_2 – коэффициент диффузии углерода (расчет мартенсита), C_{S2} – концентрация углерода на поверхности (расчет мартенсита).

C_{gl}, wt.%	C_{ch}, wt.%	T, °C	t, min	δ_p, μm	C_V, wt.%	D_1, 10^{-8} cm^2/s	C_{S1}, wt.%	δ_m, μm	C_{S2}, wt.%	D_2, 10^{-8} cm^2/s
				Pearlite layer				Martensite layer		
5	10	900	5	12	0.48	3.5±0.4	0.93	66	0.85	4.7±0.5
10	10	1000	5	12	0.56	7.8±0.8	0.86	90	0.84	8.8±0.8
10	10	900	10	26	0.69	6.8±1.7	0.95	102	1.03	4.6±0.3

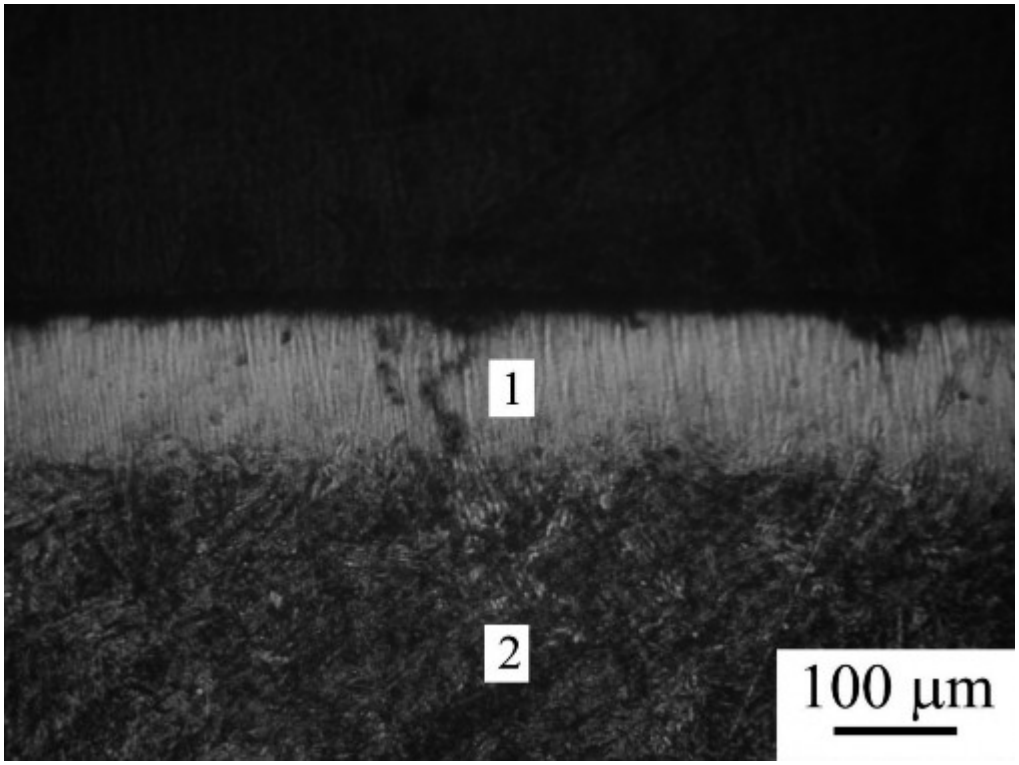

Fig. 1. The image of the cross section of low-carbon steel after its anodic PEC in an electrolyte containing 10 wt.% ammonium chloride and 10 wt.% glycerol at 900 °C for 10 min. 1 is martensitic layer, 2 is martensitic-pearlite one

Рис. 1. Изображение поперечного сечения низкоуглеродистой стали после ее анодной плазменной электролитической цементации в электролите, содержащем 10 мас.% хлорида аммония и 10 мас.% глицерина при 900 ° С в течение 10 мин. 1 – мартенситный слой, 2 –мартенситно-перлитный слой

Table 2
Таблица 2

Experimental data and results of evaluating the coefficient of carbon diffusion in various electrolytes at the anodic PEC. Nomenclature: *T* is the saturation temperature, *t* is the duration, *U* is the voltage, *I* is the current, δ_m, is the thickness of the martensitic layer, *D* is the diffusion coefficient of carbon

Экспериментальные данные и результаты оценки коэффициента диффузии углерода в различных электролитах при цементации. Номенклатура: *T* – температура насыщения, *t* – продолжительность, *U* – напряжение, *I* – ток, δ_m – толщина мартенситного слоя, *D* – коэффициент диффузии углерода

Carbon-containing component and carbon potential of corresponded electrolyte	PEC regimens				δ_m, μm	*D*, 10^{-8} cm²/s
	T, °C	*t*, min	*U*, V	*I*, A		
Acetone (0.9 %)	800	1	150	9.6	16	1.23
		3			33	1.75
		7			53	1.93
	850	1	180	7.4	42	8.5
		3			65	6.79
		7			97	6.48
	900	1	250	4.6	70	23.6
		3			102	16.71
		7			139	13.3

Continuation of table 2
Продолжение табл. 2

Carbon-containing component and carbon potential of corresponded electrolyte	PEC regimens				δ_m, μm	D, 10^{-8} cm^2/s
	T, °C	t, min	U, V	I, A		
Ethylene glycol (0.6 %)	800	1	150	12.4	6	0.28
		3			12	0.38
		7			18	0.36
	850	1	180	8.6	12	1.13
		3			18	0.84
		7			24	0.64
	900	1	210	6.8	18	2.53
		3			30	2.35
		7			42	1.97
Glycerol (0.8 %)	850	1	160	8.5	24	3.17
		3			42	3.23
		7			60	2.83
	900	1	190	6.8	30	4.95
		3			54	5.35
		7			78	4.79
	950	1	210	6.2	36	7.13
		3			72	9.51
		7			96	7.25
	1000	1	240	5.8	42	9.71
		3			84	12.90
		7			132	13.70
Sucrose (0.7 %)	850	1	170	8.6	20	2.54
		3			38	3.06
		7			54	2.65
	900	1	200	7.2	24	3.66
		3			48	4.88
		7			72	4.70
	950	1	220	6.6	30	5.72
		3			64	8.67
		7			96	8.36
	1000	1	260	6	36	8.23
		3			72	10.97
		7			114	11.79
Ethanol (0.6 %)	800	1	170	11	9	0.63
		3			15	0.59
		7			18	0.36
	850	1	200	8	12	1.13
		3			20	1.04
		7			24	0.64
	900	1	230	6.2	18	2.53
		3			28	2.04
		7			44	2.16

End of table 2
Окончание табл. 2

Carbon-containing component and carbon potential of corresponded electrolyte	PEC regimens				δ_m, μm	D, 10^{-8} cm^2/s
	T, °C	t, min	U, V	I, A		
Isopropanol (0.8 %)	800	1	160	11	18	1.78
		3			24	1.06
		7			36	1.08
	850	1	180	9	24	3.17
		3			44	3.55
		7			58	2.65
	900	1	200	7.8	32	5.64
		3			52	4.93
		7			75	4.42

Figure 2 shows the dependence of the square of the thickness of the martensitic layer on the processing time for electrolytes based on glycerol and sucrose. The obtained dependences correspond to a constant concentration of carbon on the surface of the sample. This fact indicates a rather rapid adsorption of carbon on the treated surface, which is one of the advantages of PEC.

The influence of the temperature of the PEC on the diffusion coefficient of carbon is quite standard for electrolytes containing glycerol or ethylene glycol (Fig. 3). The exponential dependence for other solutions is less pronounced, which may be associated with the growth of the oxide layer and its uncontrolled destruction.

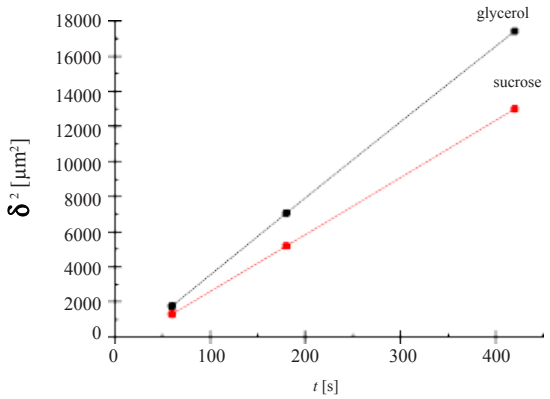

Fig. 2. The dependence of the square of the thickness of the martensitic layer on the processing time at 1000 °C in glycerol and sucrose electrolytes

Рис. 2. Зависимость квадрата толщины мартенситного слоя от времени обработки при 1000 °С в глицериновом и сахарозном электролитах

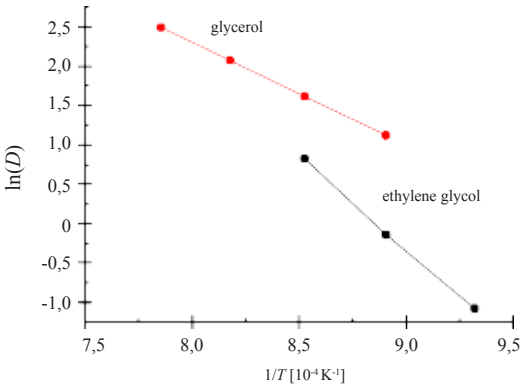

Fig. 3. The dependence of the coefficient of carbon diffusion on the temperature of the PEC in glycerol or ethylene glycol electrolytes

Рис. 3. Зависимость коэффициента диффузии углерода от температуры цементации в глицериновых или этиленгликолевых электролитах

The various carbon potentials of the studied electrolytes are related to the boiling point of carbon-containing components (56 °C for acetone and 197 °C for ethylene glycol). We also note their different densities, namely, 0.7920 g/cm3 for acetone and 1.1131 g/cm3 for ethylene glycol at 20 °C. The boiling point of these components affects the intensity of its evaporation into the VGE. The lower boiling point of acetone compared to ethylene glycol contributes to its higher concentration in the saturating medium. In addition, a lower density of acetone determines a higher mobility of the molecules in the aqueous solution, which also increases the rate of its evaporation into the VGE.

The diffusion coefficients of carbon substantially depend on the composition of the electrolyte (Fig. 4). This fact is explained by the different composition of the carburised layer. The highest values of the diffusion coefficient of carbon are reached with a minimum content of oxides in the carburised layer, inhibiting the transfer of carbon atoms. The diffusion coefficient of carbon increases by about 3 times due to an increase in the concentration of ammonium chloride, which provides more intensive anodic dissolution reducing the thickness of the oxide layer. The growth of the oxide layer with increasing temperature or saturation time, as well as with a decrease in the concentration of ammonium chloride are detected during the processing of low-carbon steel in a solution containing glycerol, ammonium chloride, and ammonium nitrate [24].

Another confirmation of the inhibitory role of the oxide layer is a decrease in the carbon diffusion coefficient as the PEC duration increases (Table 2). This trend is observed for the electrolytes containing acetone, ethylene glycol, ethanol and isopropanol, when the temperature of the PEC is high enough for a significant growth of the oxide layer. Such regularity is not revealed in glycerol and sucrose solutions which may be associated with the uncontrolled peeling off of the oxide layer.

Conclusions

1. The thickness of the martensitic layer can be used to estimate the diffusion coefficient of carbon under conditions of plasma electrolytic carburising with subsequent quenching in the same electrolyte.

2. The estimates of the diffusion coefficients of carbon in steel during anodic plasma electrolytic carburising in various electrolytes are obtained. The highest diffusion coefficient of carbon reaches $2.3 \cdot 10^{-7}$ cm^2/s (900 °C, 1 min) for an acetone-based electrolyte with minimal oxidizing ability.

3. The possibility of accelerating carbon diffusion by intensifying the anodic dissolution of the outer oxide layer inhibiting carbon diffusion is shown.

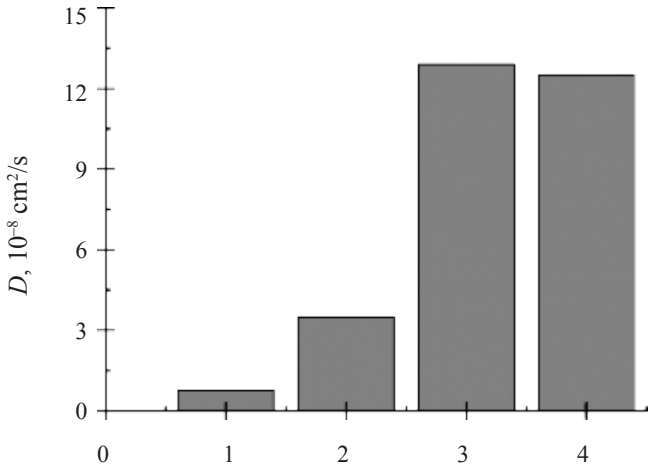

Fig. 4. The effective coefficient of carbon diffusion (10^{-8} (cm^2/s)) at the anodic PEC in various electrolytes. 1 – 10 wt.% glycerol and 10 wt.% ammonium chloride; 2 – 5 wt.% glycerol and 10 wt.% ammonium chloride; 3 – 10 wt.% glycerol and 15 wt.% ammonium chloride; 4 – 10 wt.% acetone and 10 wt.% ammonium chloride. The EPC temperature is 900 °C, the duration is 5 min

Рис. 4. Эффективный коэффициент диффузии углерода (10^{-8} (см^2/с)) при анодной цементации в различных электролитах. 1 – 10 мас.% глицерина и 10 мас.% хлорид аммония; 2 – 5 мас.% глицерина и 10 мас.% хлорид аммония; 3 – 10 мас.% глицерина и 15 мас.% хлорид аммония; 4 – 10 мас.% ацетона и 10 мас.% хлорид аммония. Температура EPC составляет 900 °C, продолжительность 5 минут.

Acknowledgments

This work was financially supported by the Russian Science Foundation (Contract No. 18-79-10094) for Kostroma State University.

References

1. Review on improving wear and corrosion resistance of steel via plasma electrolytic saturation / N. Lin et. al. // Surface Review and Letters. 2016. V. 23, No. 4. P. 1630002. DOI: 10.1142/S0218625X16300021.

2. Belkin P. N., Yerokhin A., Kusmanov S. A. Plasma electrolytic saturation of steels with nitrogen and carbon // Surface & Coatings Technology. 2016. V. 307. P. 1194–1218. DOI:10.1016/j.surfcoat.2016.06.027.

3. Yaghmazadeh M., Dehghanian C. Surface Hardening of AISI H13 Steel Using Pulsed Plasma Electrolytic Carburizing (PPEC) // Plasma Process Polym. 2009. V. 6. P. S168–S172. DOI: 10.1002/ppap.200930410.

4. Characterization of Plasma Electrolytic Carburized Stainless Steel in Glycerin Aqueous Solution / W. Xue et. al. // Journal of Aeronautical Materials. 2010. V. 30, No. 4. P. 38–42. DOI: 10.3969/j.issn.1005-5053.2010.4.008.

5. Preparation and characterization of diamond-like carbon/oxides composite film on carbon steel by cathodic plasma electrolysis / J. Wu et. al. // Appl. Phys. Lett. 2013. V. 103. P. 031905. DOI: 10.1063/1.4813830.

6. Preparation and characterization of carburized layer on pure aluminum by plasma electrolysis / J. Wu et. al. // Surface & Coatings Technology. 2015. V. 269. P. 119–124. DOI: 10.1016/j.surfcoat.2014.12.024.

7. Aliofkhazraei M., Sabour Rouhaghdam A. Neural networks prediction of different frequencies effects on corrosion resistance obtained from pulsed nanocrystalline plasma electrolytic carburizing // Materials Letters. 2008. V. 62. P. 2192–2195. DOI: 10.1016/j.matlet.2007.11.052.

8. Aliofkhazraee M., Sabour Rouhaghdam A., Shahrabi T. Pulsed nanocrystalline plasma electrolytic carburising for corrosion protection of a γ-TiAl alloy. Part 1. Effect of frequency and duty cycle // Journal of Alloys and Compounds. 2008. V. 460. P. 614–618. DOI: 10.1016/j.jallcom.2007.06.007.

9. Carburizing of low melting-point metals by pulsed nanocrystalline plasma electrolytic carburizing / M. Aliofkhazraei et. al. // Surf. Coat. Technol. 2008. V. 202. P. 5493–5496. DOI: 10.1016/j.surfcoat.2008.06.067.

10. Plasma electrolysis for surface engineering / A. L. Yerokhin et. al. // Surf Coat Technol. 1999. V. 122. P. 73–93.

11. Çavuşlu F., Usta M. Kinetics and mechanical study of plasma electrolytic carburizing for pure iron // Applied Surface Science. 2011. V. 257, No. 9. P. 4014–4020. DOI: 10.1016/j.apsusc.2010.11.167.

12. Yoshinori T. Electrolytic Thermochemical treatment // Mechanical technology. 1977. V. 25, No. 8. P. 118–119.

13. Inoue K., Yoshinori Sh. The Character of Spark Carburization // Journal of the Japan Institute of Metals. 1969. V. 33, No. 7. P. 755–760. In Japan. DOI: 10.2320/Jinstmet1952.33.7_755.

14. Weissgerber H., Bohme H., Bohme M. Elektrolytische Warmebehandlung von Stahl // Die Technick. 1969. No. 6. P. 413–417.

15. Enhanced wear and corrosion resistance of plasma electrolytic carburized layer on T8 carbon steel / J. Wu et. al. // Materials Chemistry and Physics. 2016. V. 171, No. 1. P. 50–56. DOI: 10.1016/j.matchemphys.2015.09.047.

16. Cathodic plasma electrolysis for preparation of diamond-like carbon particles in glycerol solution / J. Wu et. al. // Materials Chemistry and Physics. 2017. V. 199. P. 289–294. DOI: org/10.1016/j.matchemphys.2017.07.011.

17. Kombaev K. K., Kylyshkanov M. K., Lopukhov Yu. I.. Effect of electrolyte-plasma treatment of 18KhN3MA-Sh steel on the surface microstructure and hardness // Journal of Siberian Federal University. Engineering & Technologies. 2009. No. 4. P. 394–399. https://cyberleninka.ru/article/n/15376216.

18. Kusmanov S. A., Dyakov I. G., Belkin P. N. Influence of carbon-containing components of the electrolyte on the characteristics of electrochemical-thermal carburising // Problems of Materials Science. 2009. No. 4. P. 7–14.

19. Belikhov A. B., Belkin P. N. Features of iron-graphite anode carburizing // Surf. Eng. Appl. Electrochem. 1998. No. 6. P. 9–17.

20. Belikhov A. B., Belkin P. N. The influence of anode carburising modes on the electrical resistance of a thin wire // Surf. Eng. Appl. Electrochem. 1995. No. 2. P. 74–76.

21. Kusmanov S. A., Shadrin S. Yu., Belkin P. N. Carbon transfer from aqueous electrolytes to steel by anode plasma electrolytic carburizing // Surf. Coat. Technol. 2014. V. 258. P. 727–733. DOI: 10.1016/j.surfcoat.2014.08.005.

22. Callister W. D., Jr. and Rethwisch D. G. Fundamentals of Materials Science and Engineering. New York: John Wiley & Sons, Inc., 2007. P. 395.

23. Belkin P. N. Anodic electrochemical-thermal modification of materials based on iron and titanium // University News. Chemistry and chemical technology. 2009. V. 52, No. 2. P. 65–69.

24. Surface Modification of Low-Carbon Steels by Plasma Electrolytic Nitrocarburising / S. A. Kusmanov. et. al. // Plasma Chemistry and Plasma Processing. 2016. V. 36, No. 5. P. 1271–1286. DOI: 10.1007/s11090-016-9724-3.